

## Supplementary Material

### **Mercury patterns in lakes within a natural hotspot in the Southern Volcanic Zone of the Andes (Nahuel Huapi National Park, Patagonia, South America)**

*Carolina Soto Cárdenas<sup>A</sup>, Zaida Fernandez<sup>A</sup>, Marina Arcagni<sup>B</sup>, Andrea Rizzo<sup>B,C</sup> and María C. Diéguez<sup>A,\*</sup>*

<sup>A</sup>Grupo de Ecología de Sistemas Acuáticos a Escala de Paisaje (GESAP), Instituto de Investigaciones en Biodiversidad y Medioambiente (INIBIOMA, Universidad Nacional del Comahue–Consejo de Investigaciones Científicas y Técnicas), Pasaje Gutiérrez 1415, San Carlos de Bariloche, Río Negro, 8400, Argentina

<sup>B</sup>Laboratorio de Análisis por Activación Neutrónica (LAAN), Centro Atómico Bariloche, Comisión Nacional de Energía Atómica, Avenida Bustillo kilómetro 9.5, San Carlos de Bariloche, Río Negro, 8400, Argentina

<sup>C</sup>Centro Científico Tecnológico-Patagonia Norte, Consejo de Investigaciones Científicas y Técnicas, Avenida De Los Pioneros 2350, San Carlos de Bariloche, Río Negro, 8400, Argentina.

\*Correspondence to: Email: [dieguezm@gmail.com](mailto:dieguezm@gmail.com)

## Supplementary Methods

To characterise the CDOM fraction of the lake DOM pools, the absorbance spectra (200–800 nm) of the filtered water samples were recorded in a UV–visible spectrophotometer, at 1-nm intervals in a 100-mm quartz cuvette.

The absorption coefficients  $a_{254}$ ,  $a_{350}$  and  $a_{440}$  were calculated using the formula:

$$A_{\lambda} = a_{\lambda} \div l$$

where  $a$  is the decadal absorption coefficient ( $\text{m}^{-1}$ ),  $\lambda$  is the wavelength,  $A_{\lambda}$  is the absorbance at a given wavelength (arbitrary units AU), and  $l$  is the path length of the quartz cuvette (m). The specific UV absorbances  $a_{254}:\text{DOC}$  (SUVA; proxy for DOM aromaticity) and  $a_{350}:\text{DOC}$  (proxy for aromaticity and lignin content) were calculated following Weishaar *et al.* (2003), and Fichot and Benner (2012) respectively ( $\text{L mg}^{-1} \text{C m}^{-1}$ ). The spectral slope  $S_{275-295}$  ( $\text{nm}^{-1}$ ), typically employed as a proxy for degradation processes, was calculated by fitting the log-transformed absorbance spectral data for the interval 275–295 nm to a linear model. The  $S_{275-295}$  is inversely correlated with the DOM molecular weight, higher  $S_{275-295}$  values are indicative of low-molecular-weight CDOM (Helms *et al.* 2008, 2013; Stedmon *et al.* 2011; Fichot and Benner 2012; Hansen *et al.* 2016).

The FDOM fraction was characterised through excitation–emission matrices (EEMs) collected at specific excitation and emission intervals (Ex: 240–450 nm, Em: 300–600 nm), with the spectrofluorometer set with 10-nm excitation and emission slits and a scan speed of  $1500 \text{ nm min}^{-1}$ . Two fluorescence-based indices were calculated from the EEMs. The humifica index (HIX), used as a proxy for DOM humification degree, was calculated as the ratio of two regions of the emission scan (Em: 435–480 nm: Em300–345 nm) collected at an excitation of 254 nm (Ex: 254) (Zsolnay *et al.* 1999). Higher HIX values are indicative of increased DOM humification. The biological index (BIX) employed for the evaluation of recently produced DOM and autochthonous production, was calculated as the ratio of the emission intensities at 380 and 430 nm (Em: 380 nm and Em: 430 nm), collected at a fixed excitation of 310 nm (Ex:310 nm). High BIX values ( $>1$ ) associate with a dominant autochthonous DOM source (Huguet *et al.* 2010).

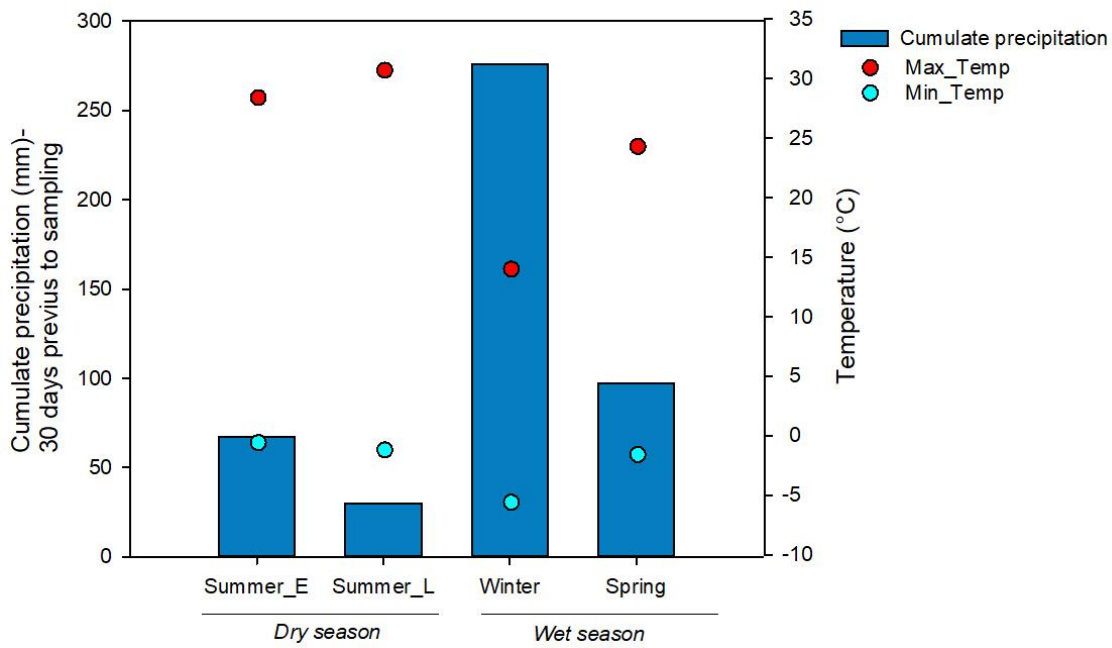


**Figure S1.** Monthly cumulative precipitation (30 days prior to sample collection date) (blue columns) and mean monthly air temperature (red circles: maximum temperature; light blue circles: minimum temperature). Data downloaded from the meteorological station “Puesto Rincón” (AIC: <http://www.aic.gov.ar/>) adjacent to the branch Brazo Rincón (BR) of Lake Nahuel Huapi. Summer\_E: December, Summer\_L: March, Winter: July, Spring: November.

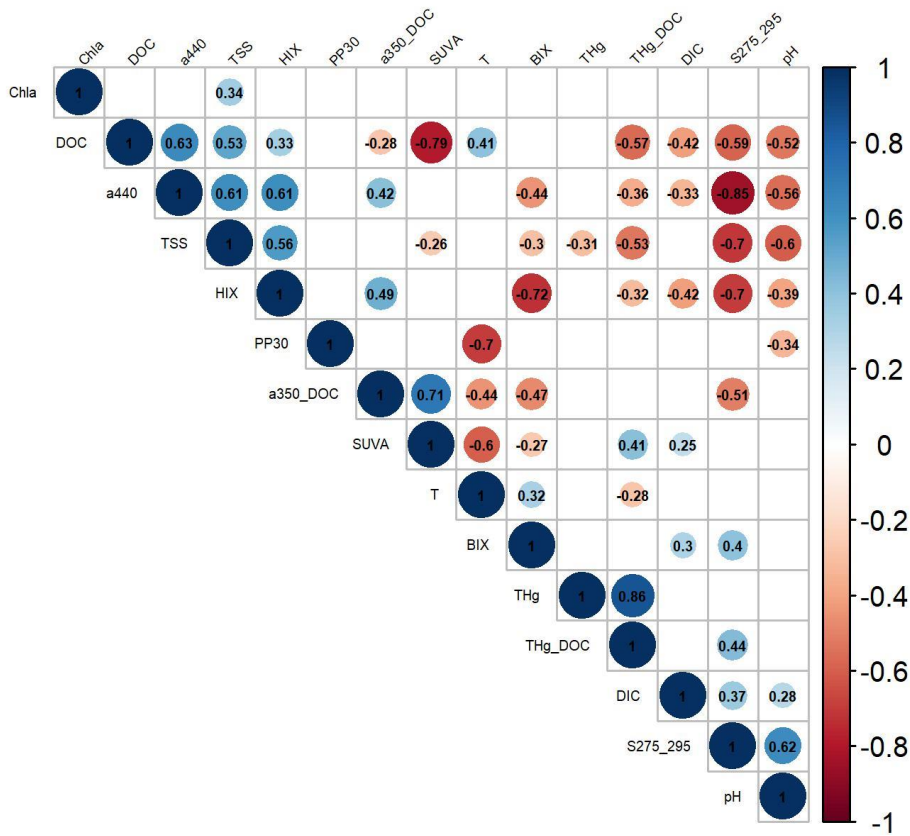


**Figure S2.** Spearman's correlation analysis of physicochemical parameters including DOM concentration and quality variables and THg concentration in the Brazo Rincón branch (BR, Lake Nahuel Huapi) and Lake Pire.

**Table S1.** Hydrogeomorphic features of Brazo Rincón branch (BR, Lake Nahuel Huapi) and Lake Pire (Nahuel Huapi National Park, Patagonia, Argentina)

	<b>Brazo Rincón branch (BR)</b>	<b>L. Pire</b>
	<b>L. Nahuel Huapi</b>	
Perimeter (km)	19.27	2.44
Area (ha)	1095	19.9
P:A (m <sup>-1</sup> )	0.0017	0.012
Z <sub>max</sub> (m)	100	20 <sup>a</sup>
DR	14.39	23.34
Catchment area (ha)	15758	464.47 <sup>A</sup>

A (lake area); P:A (lake perimeter to lake area ratio); Z<sub>max</sub> (maximum depth); DR (drainage ratio (catchment: lake area)) and catchment area.

<sup>A</sup>Mansilla Ferro *et al.* 2024.

**Table S2.** Two-way ANOVA on ranks and *post hoc* comparisons (Holm–Sidak) performed to evaluate spatial and seasonal differences in physicochemical and DOM quality variables of the lakes Pire and BR.

Variable	Two-way ANOVA		
	Factor	F	P-value
pH	Site	76.692	<0.001
	Season	6.810	<0.001
	Site*Season	5.766	0.002
Chl- <i>a</i>	Lake	4.220	0.044
	Season	0.528	0.665
	Lake*Season	1.712	0.174
DOC	Lake	147.587	<0.001
	Season	6.265	<0.001
	Lake*Season	3.548	0.020
DIC	Lake	21.909	<0.001
	Season	2.416	0.075
	Lake*Season	0.791	0.504
TSS	Lake	132.566	<0.001
	Season	0.830	0.483
	Lake*Season	0.597	0.619
Chl- <i>a</i> :TSS	Lake	87.991	<0.001
	Season	0.524	0.668
	Lake*Season	0.583	0.628
<i>S</i> <sub>275-295</sub>	Lake	147.456	<0.001
	Season	2.256	0.091
	Lake*Season	0.242	0.867
SUVA	Lake	29.778	<0.001
	Season	15.223	<0.001
	Lake*Season	3.401	0.023
<i>a</i> <sub>350:DOC</sub>	Lake	3.050	0.086
	Season	9.171	<0.001
	Lake*Season	1.146	0.338
<i>a</i> <sub>440</sub>	Lake	96.229	<0.001
	Season	6.544	<0.001
	Lake*Season	1.138	0.341
HIX	Lake	70.494	<0.001
	Season	12.709	<0.001
	Lake*Season	2.222	0.095
BIX	Lake	22.633	<0.001
	Season	41.490	<0.001
	Lake*Season	1.844	0.149
THg	Lake	10.205	0.002
	Season	2.982	0.038
	Lake*Season	13.093	<0.001
THg:DOC	Lake	61.007	<0.001
	Season	2.771	0.049
	Lake*Season	9.179	<0.001

Chl-*a*, chlorophyll-*a*; DOC, dissolved organic carbon; DIC, dissolved inorganic carbon; TSS, total suspended solids; Chl-*a*:TSS ratio, proportion of Chl-*a* in the total suspended solids; *S*<sub>275–295</sub>, spectral slope between 275 and 295 nm; SUVA, specific UV absorbance at 254 nm a 254 (*a*<sub>254</sub>),DOC); specific UV absorbance at 350 nm (*a*<sub>350</sub>,DOC); *a*<sub>440</sub>, absorption coefficient at 440 nm, color; HIX, humification index; BIX, biological index; THg, total mercury; THg:DOC, ratio of total mercury concentration to dissolved organic carbon concentration.

**Table S3.** Results of the Principal Component Analysis (PCA). Correlation coefficients of the different variables and the principal components 1, 2 and 3 (PC1, PC2 and PC3).

<b>Variables</b>	<b>PC1</b>	<b>PC2</b>	<b>PC3</b>
Precipitation (30 days)	n.s.	0.69***	-0.25**
Temp.	n.s.	-0.72***	0.08***
DOC	0.63***	-0.61***	0.3**
TSS	0.52***	-0.28**	n.s.
DIC	n.s.	-0.16***	0.62***
Chl- <i>a</i>	0.27**	n.s.	n.s.
<i>a</i> <sub>440</sub>	0.84***	0.24***	0.33***
<i>S</i> <sub>275-295</sub>	-0.9***	n.s.	-n.s.
<i>a</i> <sub>350</sub> :DOC	0.55***	0.67***	n.s.
THg	n.s.	0.27**	0.83***
BIX	-0.55***	-0.34***	0.08**
HIX	0.75***	0.27**	-0.3**
pH	-0.7***	n.s.	n.s.
THg:DOC	n.s.	0.53***	0.72***
SUVA	n.s.	0.87***	n.s.
Eigenvalue	4.15	3.3	2.02
Variance explained	27.66	21.98	13.49
Accumulated variance explained (%)	27.66	49.6	63.1

Probabilities are significant at: \*\*,  $P < 0.001$ ; \*\*\*,  $P < 0.0001$ .

**Table S4.** Results of the nonparametric PERMANOVA on Euclidean distances performed to PCA variables.

<b>Parameter</b>	<b>d.f.</b>	<b>SS</b>	<b><math>R^2</math></b>	<b><math>F</math></b>	<b><math>P</math>-value</b>
Lake	1	203.77	0.26	22.59	<b>0.001</b>
Residual	65	586.35	0.74		
Total	66	790.12	1		

Pairwise comparisons were conducted using *adonis2* in the *vegan* package.

**Table S5.** Nonparametric PERMANOVA on Euclidean distances performed to variables included in the PCA from Seasons.

<b>Parameter</b>	<b>d.f.</b>	<b>SS</b>	<b>R<sup>2</sup></b>	<b>F</b>	<b>P-value</b>
Season	3	214.33	0.27	7.82	<b>0.001</b>
Residual	63	575.79	0.73		
Total	66	790.12	1		

<b>Comparison</b>	<b>P-value</b>
Early summer v. winter	0.001
Early summer v. spring	0.001
Early summer v. late summer	0.001
Spring v. winter	0.001
Spring v. late summer	0.001
Winter v. late summer	0.001

Pairwise comparisons were conducted using `adonis2` in the *vegan* package. Only significant *a posteriori* pairwise comparisons are included.



## References

- Fichot CG, Benner R (2012) The spectral slope coefficient of chromophoric dissolved organic matter (S<sub>275–295</sub>) as a tracer of terrigenous dissolved organic carbon in river-influenced ocean margins. *Limnology and Oceanography* **57**, 1453–1466.
- Hansen AM, Kraus TE, Pellerin BA, Fleck JA, Downing BD, Bergamaschi BA (2016) Optical properties of dissolved organic matter (DOM): Effects of biological and photolytic degradation. *Limnology and Oceanography* **61**, 1015–1032.
- Helms JR, Stubbins A, Ritchie JD, Minor EC, Kieber DJ, Mopper K (2008) Absorption spectral slopes and slope ratios as indicators of molecular weight, source, and photobleaching of chromophoric dissolved organic matter. *Limnology and Oceanography* **53**, 955–969.
- Helms JR, Stubbins A, Perdue EM, Green NW, Chen H, Mopper K (2013) Photochemical bleaching of oceanic dissolved organic matter and its effect on absorption spectral slope and fluorescence. *Marine Chemistry* **155**, 81-91.
- Huguet A, Vacher L, Saubusse S, Etcheber H, Abril G, Relexans S, Ibalot F, Parlanti E (2010) New insights into the size distribution of fluorescent dissolved organic matter in estuarine waters. *Organic Geochemistry* **41**, 595–610.
- Mansilla Ferro C, Garcia PE, Reissig M, Diéguez MC (2024) Bioclimatic influence on water chemistry and dissolved organic matter in shallow temperate lakes of Andean Patagonia: A gradient approach. *Freshwater Biology* **69**, 724-738.
- Stedmon CA, Thomas DN, Papadimitriou S, Granskog MA, Dieckmann GS (2011) Using fluorescence to characterize dissolved organic matter in Antarctic Sea ice brines. *Journal of Geophysical Research: Biogeosciences* **116**, G03027.
- Weishaar JL, Aiken GR, Bergamaschi BA, Fram MS, Fujii R, Mopper K (2003) Evaluation of specific ultraviolet absorbance as an indicator of the chemical composition and reactivity of dissolved organic carbon. *Environmental Science and Technology* **37**, 4702-4708.
- Zsolnay A, Baigar E, Jimenez M, Steinweg B, Saccomandi F (1999) Differentiating with fluorescence spectroscopy the sources of dissolved organic matter in soils subjected to drying. *Chemosphere* **38**, 45-50.